

Intensity Ratios within the Balmer Lines H_α and H_β After Dissociative Excitation of C_6H_6 and H_2

H. J. Hartfuß, J. Neumann, and H. D. Schneider

I. Phys. Inst. der Justus Liebig-Universität Gießen

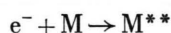
(Z. Naturforsch. **31a**, 1292–1297 [1976]; received August 30, 1976)

The decay-curves of the Balmer-lines H_α and H_β have been measured after dissociative excitation of C_6H_6 and H_2 by electron-impact in the 100 eV range. The analysis of the decay-curves shows, in agreement with other authors, that only the 3s- and 3d-states in the case of H_α and the 4s- and 4d-states in the case of H_β contribute significantly to the total intensity of H_α and H_β , respectively, but not the p-states 3p and 4p.

The intensity-ratios $J(3s)/J(H_\alpha)$ and $J(4s)/J(H_\beta)$ have been investigated. Comparison with the total emission cross-sections of the states $n=3$ and $n=4$ allows to determine the excitation cross-sections of the sublevels 3s and 4s. It is found that s-state production is favoured in the dissociation process. This seems to be independent on the principal quantum number.

I. Introduction

It has been shown by several authors¹ that electron impact on hydrocarbon-molecules produces so-called super-excited-states, which in our case are optically forbidden with respect to the molecular ground-state. Molecules in these states with energies above the ionization-potential of the molecules show preionisation and dissociation. In the latter case excited atoms may be produced. Thus, after electron-impact on hydrogen-containing molecules the Balmer-lines can be observed:



The emission cross-sections of the Balmer-lines H_α to H_δ are known for a variety of hydrocarbons as a function of electron energy^{2,3}. But the techniques applied allowed only to determine total the cross-sections of the H-states $n=3$ to $n=6$ and not those of the sublevels $l=0$ to $l=n-1$.

Because of the n -fold l -degeneracy of the hydrogenstates with principal quantum-number n ¹⁹, the total intensity of the Balmer-lines is composed of three parts, corresponding of the transitions $ns-2p$, $np-2s$ and $nd-2p$ ($n>2$).

These three transitions have significantly different total transition-probabilities⁴. Therefore a good separation of the different decay-components and the determination of their relative portions is possible by registering the Balmer-decay.

Making use of this fact, Weaver and Hughes⁵ determined the intensity of the H_α -emission, starting

Reprint requests to Dr. H. J. Hartfuß, I. Physikalisches Institut der Universität Gießen, D-6300 Gießen.

from the 3s- and 3d-sublevels relative to the total intensity of the H_α -line after dissociative excitation of H_2 by electron-impact. Recently Tsurubuchi, Möhlmann and de Heer⁶ extended this kind of measurement on other hydrogen-containing molecules (HCl , H_2O , NH_3 , CH_4).

One of us⁷ has carried out decay measurements of the Balmer-lines H_α to H_δ after dissociative excitation of C_6H_6 and C_6D_6 , but with deviating results. The present series of measurements was started to solve these discrepancies. We intend to prove the statement of⁷ that all the Balmer-lines show essentially equal decay-behaviour. This was explained by a common production-mechanism for the excited fragments, which should reflect certain molecular features.

Variation of the target-molecules should give an answer to this question. Therefore, beside C_6H_6 the decay-behaviour of the first two Balmer-lines after dissociative excitation of H_2 has been studied. Believing to be able to explain the deviations, we give on this basis the results of measurements on C_6H_6 and H_2 . The measurements on H_2 are in good agreement with those of Tsurubuchi et al.⁶

II. Apparatus

A crossed-beam experiment was built up consisting of an electron- and molecular-beam as described in detail in Reference⁸. The electron-beam is switched by a pulse of 300 ns duration and a repetition-rate of about 300 kHz. The decay-time of the excitation-pulse is 4.8 ns. The decay-curves have been registered by the method of delayed coincidences using a time-to-height converter and a multi-



Dieses Werk wurde im Jahr 2013 vom Verlag Zeitschrift für Naturforschung in Zusammenarbeit mit der Max-Planck-Gesellschaft zur Förderung der Wissenschaften e.V. digitalisiert und unter folgender Lizenz veröffentlicht: Creative Commons Namensnennung-Keine Bearbeitung 3.0 Deutschland Lizenz.

Zum 01.01.2015 ist eine Anpassung der Lizenzbedingungen (Entfall der Creative Commons Lizenzbedingung „Keine Bearbeitung“) beabsichtigt, um eine Nachnutzung auch im Rahmen zukünftiger wissenschaftlicher Nutzungsformen zu ermöglichen.

This work has been digitalized and published in 2013 by Verlag Zeitschrift für Naturforschung in cooperation with the Max Planck Society for the Advancement of Science under a Creative Commons Attribution-NoDerivs 3.0 Germany License.

On 01.01.2015 it is planned to change the License Conditions (the removal of the Creative Commons License condition "no derivative works"). This is to allow reuse in the area of future scientific usage.

channel-analyzer. Compared to ⁸ only little was varied, concerning especially the electron-beam-collimation. Besides we have changed from graphical to computer-evaluation of the data by a least-squares fit. The essential conditions of the experiment are unchanged: $I_{\max} = 100 \mu\text{A}$ between 100 and 500 eV, the max. density of the molecular beam in its forward direction corresponding to about $5 \cdot 10^{-4}$ Torr, background-pressure $1 \cdot 10^{-6}$ Torr. One detail has turned out to be very influential: The diameter of the electron-beam is about 2 mm. Its luminescing trace when passing the molecular-beam is projected by a lense in twice the focal distance to the entrance slit ($300 \mu\text{m}$) of the 0.25 m-monochromator.

This causes a restriction of the observable region in the plane of the electron- and molecular-beam to a small window of 5...6 mm width by 14 mm length. Errors introduced by this arrangement will be explained together with the discussion of the results (IV. 1).

III. Evaluation of the Data

A decay-curve measured by the method of delayed coincidences is given in Figure 1. As men-

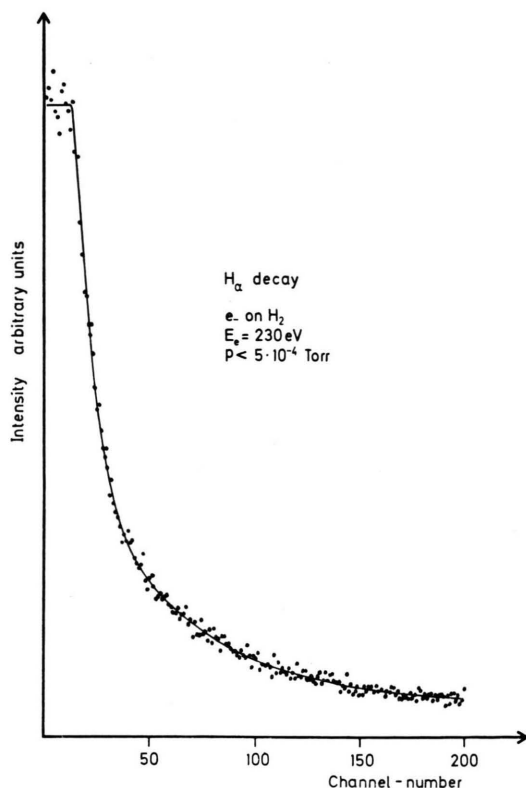


Fig. 1. Example of a measured decay-curve (points) and the fit (drawn curve) as described in Part III.

tioned above the curves are analyzed by a non-linear regression computation with the computer-program BMDX 85⁹. (Drawn curve in Figure 2.) The total decay of the Balmer-lines consisting of three independently decaying components, starting from the states ns, np and nd, is given by three exponentials:

$$J(t) = J_0^s \cdot e^{-t/\tau_s} + J_0^p \cdot e^{-t/\tau_p} + J_0^d \cdot e^{-t/\tau_d}. \quad (1)$$

To describe the measured curves exactly, some corrections have to be made concerning the time-independent background, caused by the intense continuum, covering the whole visible wavelength-region starting at about 3000 \AA ⁷. Moreover dark pulses of the cooled photomultiplier contribute to the background. Furthermore we have to consider the finite decay of the excitation pulse, which is exponential within the first 1.5 decades of decay with a time-constant of 4.8 ns: The number of excited atoms N , having the lifetime τ and the stationary population N_0 given by

$$\text{const } \sigma N_G J_0 - \frac{1}{\tau} N_0 = 0$$

decays, with $J = J_0 e^{-t/\tau_A}$ ($t > 0$), according to the equation

$$dN/dt = (1/\tau) N_0 e^{-t/\tau_A} - (1/\tau) N$$

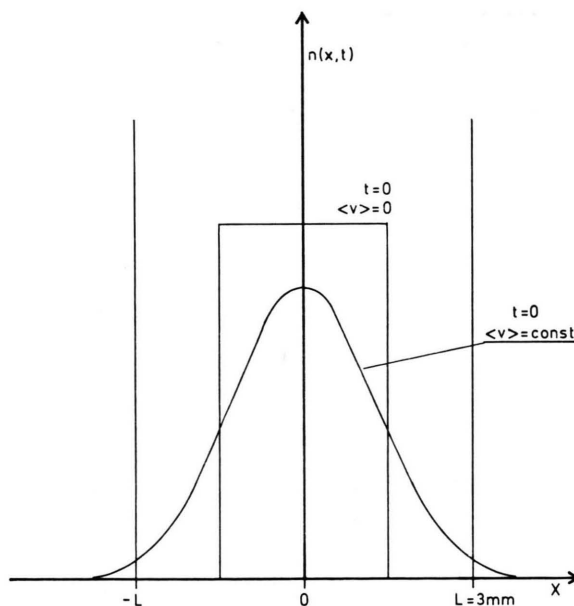


Fig. 2. Sketch to explain the observation-conditions in this experiment (Part IV.1).

with the solution

$$N(t) = \frac{N_0}{\tau - \tau_A} \{ \tau e^{-t/\tau} - \tau_A e^{-t/\tau_A} \}. \quad (2)$$

For each of the Balmer-components such a solution holds, so that the total decay can be described by

$$J(t) = \sum_{n=s,p,d} \frac{J_0^n}{\tau_n - \tau_A} \{ \tau_n e^{-t/\tau_n} - \tau_A e^{-t/\tau_A} \} + U. \quad (3)$$

First of all the computer-fit determined the intensities J_0^s , J_0^p , J_0^d , and U together with the decay-times τ_s , τ_p , τ_d . J_0^p proved to be most often zero or very near zero. Considering the so-called dynamical intensities, which result if one state (n, l, m) is created per second:

$$J_{nl}^{n'l'} \sim (2l+1) \frac{A_{nl}^{n'l'}}{\sum_{n'l'} A_{nl}^{n'l'}}$$

the Balmer α - and Balmer β -components should have intensities and relative amounts as listed in Table I.

Table I. Dynamical intensities as given by

$$J_{nl}^{n'l'} = (2l+1) \frac{A_{nl}^{n'l'}}{\sum_{n'l'} A_{nl}^{n'l'}} h \nu_{nl}^{n'l'}.$$

l	n		$J(3p)/J(H_\alpha) = 0.06$ $J(3s)/J(H_\alpha) = 0.16 = R_\alpha^{\text{th}}$
	3	4	
s	3.0	2.3	$J(4p)/J(H_\beta) = 0.08$
p	1.06	1.42	$J(4s)/J(H_\beta) = 0.12 = R_\beta^{\text{th}}$
d	15	15	

Under our special excitation conditions the intensity-ratios of the longer-living components (3s, 4s) are significantly greater, those of the short components (3p, 4p) smaller than the dynamical intensities. Therefore all decay-curves are fitted to only two exponentials.

IV. Results

IV.1. Discussion of Systematic Errors

The results obtained by repetition of the measurements on C_6H_6 confirmed the earlier results: The decay-curve consisted of two components whose shorter one had about the theoretical lifetime of the 3d-state of 15.6 ns and that of the 4d-state of 36.5 ns, respectively. On the other hand the longer component did not have the theoretical value of the

3s-state of 160 ns and that of the 4s-state of 230 ns but was significantly shortened depending on the target-molecule used.

The reason for this shortening was not understood. Collision-quenching could not be responsible because of the low pressure used ($< 5 \cdot 10^{-4}$ torr).

As has been shown in ¹¹ and ¹² electrical fields caused by charging of the collision chamber or caused by space-charge as the result of high current-density of the electron-beam can introduce an additional transition-probability. Only very low field-strengths are necessary to mix the extremely densely spaced (Lamb-shift) hydrogen-states with $l = j \pm 1/2$ (for example $3s_{1/2}$, $3p_{1/2}$). This mixing considerably changes the decay-behaviour especially of the long living s-states. Critical field-strengths, where the decay of both the states is entirely assimilated, are only a few V/cm. But a variation of the current-density and/or the beam-collimation led only to unsystematic changes, but not to any lengthening. To avoid charging of the collision-chamber, this was gold-plated one time and sooted another time. The same was done with the collimation-electrodes and the Faraday-cage. But no change was found. Concerning the space-charge, an approximation with the formulas given by Purcell ¹³ shows that it could not be responsible for the drastical shortening of the 3s- and 4s-lifetimes: Under the assumption that the electrons and the ions produced form an electrically neutral plasma, we get at our mean electron-energy of 200 eV and our current-density of 1.6 mA/cm² an ion density of $1.2 \cdot 10^7/\text{cm}^3$. After Purcell concentrations of $3.1 \cdot 10^8/\text{cm}^3$ and $6.2 \cdot 10^7/\text{cm}^3$ respectively are necessary to shorten the lifetimes of the 3s- and 4s-states by 15%. Thus our 30 to 50% cannot be explained this way. The reason must be of different nature.

Lamb and Sanders ¹⁴ and recently Freund et al. ¹⁵ determined from the observed Doppler-width of the Balmer-lines the kinetic energy of the excited fragments after dissociative excitation of H_2 by fast electrons. They found values up to 6 eV [much higher energies are thinkable in some possible dissociation mechanisms of H_2 (16)]. The high fragment velocities must lead in our experiment to a loss of excited H-atoms by diffusion out of the observation-region, causing a shortened decay.

Imaging the observation-region limited by two infinite planes parallel to the plane of e⁻-beam and the direction of observation with a distance of $L =$

5, ..., 6 mm, the width of the observation-window, the time-dependent decrease of the excited-particle-density between the planes has to be found.

The electron-beam produces a cylindrical distribution of 2 mm diameter of excited particles, increasing like $1 - e^{-t/\tau}$. Using the fragment-velocities of Freund¹⁵ of about $2.7 \cdot 10^6$ cm/s an essential amount of excited molecular fragments reaches the limiting planes in about 200 to 300 ns. After this time the excitation is switched off ($t=0$). The total number of excited particles within the observation window decays via two channels, natural-decay and diffusion.

The time-dependent intensity decay will be described by the product of $I(t)$, the time-dependent terms of Eq. (3) and the function $D(t)$, which describes the diffusion-process: We use the solution of the time-dependent diffusion-equation, solved under the starting-condition of a rectangular initial density-distribution between infinite parallel planes through which the particles diffuse¹⁸:

$$n(x, t) = \sum_k F_k \cdot \cos\left(\frac{x}{L} (2k-1)\pi\right) \cdot e^{-A_k t}.$$

Because in our case at $t=0$ the distribution is smeared out extensively, in a rough approximation only the first term of the series is used (approximation of the density-distribution at $t=0$ by a cosine-function). So the function $D(t)$ is given by a single exponential with an exponent containing a factor of geometry and the diffusion-constant, which is proportional to the mean-velocity $\langle v \rangle$ of the excited fragments.

Because only time-dependend processes are regarded, the time-independend factor does not play any role, so

$$D(t) = e^{-t \cdot A_d}.$$

Fitting the measured decay-curves, the theoretical values τ_s , τ_d and the measured τ_A are substituted into Equation (3). The parameters J_0^s , J_0^d , U and the diffusion constant A_d are determined by the fit. Because A_d is proportional to $\langle v \rangle$ of the excited H-atoms, the observations of⁷ can be explained.

Measurements with a filter-photomultiplier-combination confirms the validity of the approximation: We found the theoretical lifetimes of the ns-states (160, 230 ns) and the same intensity-ratios as with the lens-monochromator-arrangement (Table II). This is evidence for the assumption that after the

excitation-time of 300 ns no significant amount of the long-living fast fragments has left the observation-region.

Because in the case of the 160 ns- and the 230 ns-components no equilibrium is reached after the excitation-time of 300 ns, the measured intensities at $t=0$ are corrected by $(1 - e^{-300/\tau_s})^{-1}$.

Table II. The intensity-ratios $J(3s)/J(H_\alpha)$ and $J(4s)/J(H_\beta)$ after dissociative excitation of H_2 and C_6H_6 .

Molecule	This work	Other work	A_d ($10^6/\text{sec}$)
$J(3s)/J(H_\alpha) = R_\alpha$			
H_2	0.40 ± 0.03	0.39 ± 0.04^a	4.6 ± 0.7
	0.37 ± 0.01^c	0.24^b	
C_6H_6	0.62 ± 0.04		3.9 ± 0.6
$J(4s)/J(H_\beta) = R_\beta$			
H_2	0.30 ± 0.02	0.14^b	4.7 ± 0.4
C_6H_6	0.42 ± 0.02		2.4 ± 0.6
	0.41 ± 0.01^c		

^a Ref. ⁶. ^b Ref. ⁵. ^c Filter-measurement.

IV. 2. Intensity-ratios

In the energy-range 110 to 440 eV 10 measurements have been carried out on each of the H_α and the H_β -lines after dissociative excitation of H_2 , 8 on H_α and 11 on H_β after dissociative excitation of C_6H_6 .

Besides statistical fluctuations, no significant change of the measured ratios with impact energy was found. Table II gives the mean values of our measurements in comparison to the results of other groups. The errors given are mean square deviations from the mean value.

It is obvious that good agreement exists between our measurements and those of Tsurubuchi et al.⁶. The ratios given by Weaver and Hughes⁵ are strongly deviating from ours. Some reasons can be found which may cause the deviation. But they should shorten the lifetimes, which was not observed. The discrepancies are therefore still not understood.

Cascading is neglected in the papers mentioned as it should not play an important role: Considering first of all the H_α -line and by turn the states 3s, 3p, 3d and the possibilities to populate these states via cascades, 3s can only be populated by the higher np-states. No change of the measured life-times should be observed because of the short decay-time even of the higher p-states ($n > 4$). Moreover, because of the unfavourable branching-ratios, $np \rightarrow 3s$

cascades can not play a role, as only about 3% of these np -states decay via IR-Emission.

The $3p$ -state can be populated via nd - and ns -states ($n \geq 4$). About 24% of the nd - and between 28 and 42% of the ns -depopulation happens via $3p$. But only 11.8% of the $3p$ -states produced in this way contribute to Balmer-emission. Therefore, this portion is just at the indication-limit. It should occur – if not as a new decay-component with the decay-time of the starting-level of the cascade which is 36, 70 or 127 ns for the three higher nd -levels, and 230, 360, and 570 ns for the higher ns -levels – as an apparent lengthening of the $3d$ -component or as an apparent lengthening of the $3s$ -decay-component, because such a manifold of decay-components is not resolvable any more. But we find in our filter-measurements with good accuracy the theoretical lifetimes of the $3d$ - and $3s$ -states, so this cascade can be neglected, too.

The same is true for cascades originating in the nf -states whose decay-times of 73, 140, and 243 ns ($n = 4, \dots, 6$) should lengthen the decay-time of the $3d$ -state.

The population of $3d$ via np -states can be eliminated again like that of the $3s$ -states because of the branching-ratios. Similar conditions hold for the Balmer-line H_β : Significant errors should arise only in the case of $4d$ -population via $5f$ (37%) and $6f$ (31%) because the lifetime of the $6f$ -state of 243 ns is very close to that of the $4s$ -state, so $4d$ may pretend additional $4s$ -amounts. The intensity-ratios ($J(4s)/J(H_\beta)$) found by analyzing the decay-curves would therefore be too large.

We think the excitation probability of the nf -states to be not particularly high, otherwise they would have appeared in the H_α -emission as mentioned above. Summarizing, errors introduced by cascading are as low as a few per cent.

The relative intensity-ratios $J(3s)/J(H_\alpha)$ and $J(4s)/J(H_\beta)$, found in this experiment are significantly larger than the corresponding dynamical intensity-ratios listed in Table I.

Evidently the states with zero-angular-momentum are preferred by the dissociation-processes: Comparing the measured ratios in the H_2 -case

$$\frac{J(3s)}{J(H_\alpha)} = R_\alpha^{H_2}$$

with the corresponding theoretical ratio R_α^{th} from Table I, we find that $R_\alpha^{H_2} = (2.5 \pm 0.2) R_\alpha^{th}$. Form-

ing the same ratio for $n = 4$, we get

$$R_\beta^{H_2} = (2.5 \pm 0.2) \cdot R_\beta^{th}$$

which means that the ratios $R_\alpha^{H_2}$ and $R_\beta^{H_2}$ are both greater by the same factor than the corresponding theoretical ratios independent of the Balmer-line under investigation. Doing the same with the C_6H_6 -ratios, one finds:

$$R_\alpha^{C_6H_6} = (3.9 \pm 0.25) R_\alpha^{th}$$

for $n = 3$ and

$$R_\beta^{C_6H_6} = (3.5 \pm 0.2) \cdot R_\beta^{th}$$

in the case of $n = 4$.

The latter do not agree as well as the ratios derived in the H_2 -case, but it seems that the s -state-production is preferred by the same factor which does not depend on the principal quantum number, but only on the target-molecule used.

Unfortunately no theoretical predictions exist concerning absolute values of the ratios as well as their dependence on the principal quantum number, so no comparison is possible. To decide whether the assumption is right or not, more information is needed. Systematic variations are just being carried out at this laboratory.

IV. 3. Fragment-velocities

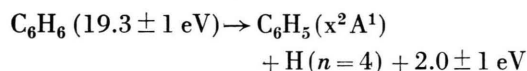
The values of the diffusion-constant A_d , listed in Table II, allows to determine mean velocities of the excited fragments. Because $A_d = \text{const} \cdot \langle v \rangle$, where the constant depends only on the geometry of the arrangement, relations between the excited particle-velocities after the fragmentation of H_2 and C_6H_6 respectively can be given.

The values of A_d for H_α and H_β for the dissociative excitation of H_2 are nearly equal. Those of H_α and H_β for dissociative excitation of C_6H_6 differ from each other and are both significantly lower than the corresponding value in the H_2 -case.

This means that the velocities of the excited H-atoms after the excitation of C_6H_6 are lower by a factor of 2.4/4.6 and 3.9/4.6, respectively.

Recently Khayralla¹⁶ and Freund et al.¹⁵ discussed the processes which lead to the fragmentation of H_2 and to the production of excited H-atoms. Both derived mean energies of the fragments and the latter group measured them to be up to 6 eV for a considerable amount. Taking a mean value of about 4 eV for the H_2 -case and evaluating A_d , we get for the mean kinetic energy of the Balmer α - and β -emit-

ting atoms 1.1 ± 0.6 eV for $H(n=4)$ -atoms and 2.8 ± 0.9 eV for $H(n=3)$ -atoms respectively after the excitation of C_6H_6 . Beenakker² supposed a single process to be responsible for the production of $H(n=4)$ -atoms after electron-impact on C_6H_6 whose threshold-energy is 19.3 ± 1 eV:



at which the dissociation-energy of the C–H-binding is taken to be 4.6 eV. The value for the residual kinetic energy is within the limits of error in good agreement with our value of 1.1 ± 0.6 eV. If the process is responsible for the production of $H(n=3)$ -atoms, too, the kinetic energy of the H_α -emitting atoms would be higher by the energy difference $E[H(n=4)] - E[H(n=3)] = 0.7$ eV.

Taking again Beenakkers value of 2.0 ± 1 eV for the $H(n=4)$ -atoms, our value of 2.8 ± 0.9 eV for $H(n=3)$ -atoms would agree very well considering the energy difference of 0.7 eV. But our two values of 1.1 ± 0.6 eV and 2.8 ± 0.9 eV differ from each other by more than 0.7 eV if one does not consider the error bars. This may be due to the rough approximation used to describe the diffusion-processes, or to the relatively uncertain value for the mean energy of the H-atoms after the fragmentation of H_2 , which was taken as reference.

IV. 4. Cross-sections

The intensity-ratios given in Table II allow to derive excitation cross-sections for the production of

H-atoms in the 3s- and 4s-states. To do this, the total emission cross-section measured by Vroom and de Heer^{2, 17} are used:

$$\sigma_{3s} = \sigma_{\text{total}} \cdot J(3s)/J(H_\alpha)$$

equivalently for $n=4$, but considering the branching ratio. Because the intensity-ratios $J(3s)/J(H_\alpha)$ and $J(4s)/J(H_\beta)$ do not vary with impact-energy between 100 and 500 eV, it is sufficient to consider the total emission cross-sections at a single, fixed energy, for instance at 200 eV. Vroom and de Heer found $6.06 \cdot 10^{-19} \text{ cm}^2$ for Balmer α and $1.1 \cdot 10^{-19} \text{ cm}^2$ for Balmer β after the dissociative excitation of H_2 . The corresponding values for C_6H_6 are $33.2 \cdot 10^{-19} \text{ cm}^2$ for H_α and $5.95 \cdot 10^{-19} \text{ cm}^2$ for H_β . From this Table III is derived.

Table III. Excitation cross-sections in units of 10^{-19} cm^2 as derived with the ratios of Table II and the total emission cross-sections from Ref.^{3, 17} for the dissociative excitation of H_2 and C_6H_6 by 200 eV-electrons.

	3s	4s
H_2	2.4 ± 0.2	0.57 ± 0.04
C_6H_6	20.7 ± 1.2	4.3 ± 0.2

Acknowledgement

We are grateful to Prof. Dr. A. Schmillen for many helpful discussions and the critical reading of the manuscript, furthermore to Prof. Dr. A. Scharmann for his stimulating interest and the Deutsche Forschungsgemeinschaft for financial support.

¹ F. J. de Heer, Int. J. Radiat. Phys. Chem. **7**, 137 [1975] and references therein.

² C. I. M. Beenakker, Thesis University of Leiden [1974].

³ D. A. Vroom and F. J. de Heer, J. Chem. Phys. **50**, 573 [1969].

⁴ H. A. Bethe and E. E. Salpeter, Quantum mechanics of One- and Two-Electron Atoms, Berlin 1957.

⁵ L. D. Weaver and R. H. Hughes, J. Chem. Phys. **52**, 2299 [1970].

⁶ S. Tsurubuchi, G. R. Möhlmann, and F. J. de Heer, Chem. Phys. Lett. to be published.

⁷ H. J. Hartfuß, Z. Naturforsch. **29 a**, 1431 [1974].

⁸ H. J. Hartfuß, Z. Naturforsch. **29 a**, 1489 [1974].

⁹ W. J. Dixon, BMD-Computer Programs, Univ. of Calif., Press Berkeley, 1970.

¹⁰ H. J. Hartfuß, Thesis, University of Gießen 1974.

¹¹ L. R. Wilcox and W. E. Lamb, Phys. Rev. **119**, 1915 [1960].

¹² L. D. Weaver, Thesis, University of Arkansas 1970.

¹³ E. M. Purcell, Astrophys. J. **116**, 457 [1952].

¹⁴ W. E. Lamb and T. M. Sanders, Phys. Rev. **119**, 1901 [1960].

¹⁵ R. S. Freund, J. A. Schiavone, and D. F. Brade, J. Chem. Phys. **64**, 1122 [1976].

¹⁶ G. A. Khayrallah, Phys. Rev. A **13**, 1989 [1976].

¹⁷ D. A. Vroom and F. J. de Heer, J. Chem. Phys. **50**, 580 [1969].

¹⁸ J. B. Hasted, Physics of Atomic Collisions, London 1972.

¹⁹ This is only true in a non relativistic approximation.